Molecular Mechanics Simulations of Thermodynamic Functions and Infrared Spectra of Alkanes

Yoshihisa Miwa and Katsunosuke Machida*

Contribution from the Faculty of Pharmaceutical Sciences, Kyoto University, Sakyo-ku, Yoshida, Kyoto 606, Japan. *Received October 16, 1987*

Abstract: An empirical molecular potential function of alkanes was constructed with the purposes of calculating the equilibrium structure, the thermodynamic functions, and normal frequencies and of simulating the infrared spectra. The potential function includes the pairwise interaction terms between nonbonded atoms, the bond-stretching terms given by the Morse function, and the quadratic valence force terms of the diagonal bend-bend type and the off-diagonal stretch-stretch, stretch-bend, and bend-bend types. The single cosine term for each dihedral angle was added to this potential function. The pairwise interaction terms consist of the exchange repulsion-dispersion potential in an approximate exp-6 type and the Coulomb potential between flexible atomic charges. The atomic charges and their derivatives with respect to internal coordinates are commonly used as the infrared intensity parameters and the Coulomb potential parameters. The calculated thermodynamic functions and structure parameters of normal and branched alkanes agree well with the experimental values. The calculated infrared spectra of *all-trans-n*-alkanes correspond well to the observed spectra in the solid state. The infrared spectra of *n*-hexane and *n*-heptane in the liquid state at room temperature are simulated successfully by using the populations of their rotational isomers calculated from the free energy differences.

Molecular mechanics calculations have been widely used for the studies of molecular structures and conformational energies.[1] Some of the model force fields so far designed to predict these molecular properties have also been adapted for the use in normal-coordinate analyses.[2-6] The ability to predict normal frequencies is essential for any force fields from which the temperature dependence of the thermodynamic functions is to be calculated correctly. Since the experimental assignment of fundamental frequencies is often misled by the lack of knowledge on the transition probability, it is desirable to extend the molecular mechanics calculation further to the direct simulation of vibrational spectra under the harmonic approximation. To pursue this purpose, however, construction of the model force field should be reconsidered from the standpoint of the self-consistency, which requires us to incorporate the atomic charges derived from the infrared band intensities as parts of the potential parameters. An empirical force field built up in this way is qualified as an object of the direct comparison with a given ab initio force field, since any molecular properties derivable from the latter are also derivable from the former in principle.

Recently, Gussoni et al. have carried out successful calculations of the infrared intensities of alkanes from the bond dipole moments and their derivatives with respect to the related internal coordinates (electrooptical parameters) and calculated the atomic charges and their fluxes on the change of internal coordinates from these parameters.[11-16] Combining a simplified set of charges and charge fluxes of these authors with the method of molecular mechanics, we have tried to simulate the infrared spectra of simple alkanes in thermal equilibria in this work. The nonadditivity of bond energies in the heats of formation of normal and branched alkanes was elucidated from the Coulomb potential between the atomic charges. The proposed potential predicts the change of structure parameters on the cyclization to form six- to eight-membered rings. Results of the simulation of Raman spectra of *n*-alkanes by using the same potential model are reported elsewhere.[17]

Procedure

Potential Functions and Parameters. The potential energy of an alkane molecule measured from the level of a completely dissociated assembly of its constituent atoms is expressed in eq 1 where r_i^0 and θ_j^0 are

$$V = \sum_i D_i^e \exp\{-a_i(r_i - r_i^0)\}[\exp[-a_i(r_i - r_i^0)] - 2] + \sum_j \tfrac{1}{2}H_j(\theta_j - \theta_j^0)^2 + \sum_{i,j} F_{ij}(r_i - r_i^0)(r_j - r_j^0) + \sum_{i,j} F_{ij}(r_i - r_i^0)(\theta_j - \theta_j^0) + \sum_{i,j}(\theta_i - \theta_i^0)(\theta_j - \theta_j^0) + \sum_i V_t(\tau_i) + \sum_{i,j} \tfrac{1}{2}V_{Nb}(r_{ij}) + \sum_{i,j} \tfrac{1}{2}q_iq_j(1/\epsilon_{ij}r_{ij}) \quad (1)$$

the intrinsic equilibrium values of the ith bond length and the jth valence angle, respectively, r_i and θ_j being the corresponding instantaneous values, and r_{pq} is the distance between the atoms p and q. The terms in the first sum in eq 1 represent the Morse potentials for the stretching coordinates, D_i^e being the dissociation energy from the potential minimum. The second through the fifth sums represent a general valence-type quadratic potential. The second sum consists of the diagonal terms of the valence angle bending coordinates. The third sum gives the stretching-stretching interaction terms taken only for the pairs that share an atom. The fourth and fifth sums are the stretching-bending and bending-bending interaction terms, respectively, both taken for the pairs that share two atoms. The sixth sum includes the torsional potential for every dihedral angle around a single bond jk, τ_{ijkl}, in the form of eq 2. The seventh and the

$$V_t(\tau_{ijkl}) = \tfrac{1}{2}v_3(1 + \cos 3\tau_{ijkl}) \quad (2)$$

last sums in eq 1 are the exchange repulsion-dispersion potential and the Coulomb potential, respectively, between nonbonded atomic pairs. The Buckingham exp-6 type potential (eq 3) has been widely used as the

$$V_B(r_{ij}) = B_{ij} \exp(-C_{ij}r_{ij}) - A_{ij}/r_{ij}^6 \quad (3)$$

former in the molecular mechanics calculations[4-10] and the lattice dynamical studies.[18] However, the energy calculated by eq 3 goes down to negative infinity in the range of small r_{ij} and makes it difficult to search for the equilibrium geometry. To avoid such trouble, we intro-

(1) Burkert, U.; Allinger, N. L. *Molecular Mechanics*; American Chemical Society: Washington, DC, 1982.
(2) Lifson, S.; Warshel, A. *J. Chem. Phys.* **1968**, *49*, 5116.
(3) Ermer, O.; Lifson, S. *J. Am. Chem. Soc.* **1973**, *95*, 4121.
(4) Chang, S.; McMalley, D.; Shary-Tehrany, S.; Hickey, S. M. J.; Boyd, R. M. *J. Am. Chem. Soc.* **1970**, *92*, 3109.
(5) Fitzwater, S.; Bartell, L. S. *J. Am. Chem. Soc.* **1976**, *98*, 5107.
(6) Wertz, D. M.; Allinger, N. L. *Tetrahedron* **1979**, *35*, 3.
(7) Allinger, N. L. *J. Am. Chem. Soc.* **1977**, *99*, 8127.
(8) Dosen-Micovic, L.; Jeremic, D.; Allingr, N. L. *J. Am. Chem. Soc.* **1983**, *105*, 1716.
(9) Engler, E. M.; Andose, J. D.; Schleyer, P. v. R. *J. Am. Chem. Soc.* **1973**, *95*, 6802.
(10) Jaime, S.; Osawa, E. *Tetrahedron* **1983**, *39*, 2769.
(11) Gussoni, M.; Abbate, S.; Zerbi, G. *J. Chem. Phys.* **1979**, *71*, 3428.
(12) Gussoni, M.; Abbate, S.; Dragoni, B.; Zerbi, G. *J. Mol. Struct.* **1980**, *61*, 355.
(13) Gussoni, M.; Abbate, S.; Sanvito, R.; Zerbi, G. *J. Mol. Struct.* **1981**, *75*, 177.
(14) Gussoni, M.; Jona, P.; Zerbi, G. *J. Chem. Phys.* **1983**, *78*, 6802.
(15) Gussoni, M.; Castiglioni, C.; Zerbi, G. *J. Phys. Chem.* **1984**, *88*, 600.
(16) Gussoni, M. *J. Mol. Struct.* **1984**, *113*, 323.
(17) Machida, K.; Noma, H.; Miwa, Y. *Indian J. Pure Appl. Phys.* **1988**, *26*, 197.
(18) Kobayashi, M. *J. Chem. Phys.* **1978**, *68*, 145. Kobayashi, M. *Ibid.* **1979**, *70*, 509, 4797.

0002-7863/88/1510-5183$01.50/0

duced an approximate form of eq 3 by rewriting the repulsion term as a product of an inverse power and a Lorentzian function (eq 4). This

$$V_{Nb}(r_{ij}) = \frac{b^2}{(r_{ij} - r_m)^2 - b^2}\left(\frac{r_m}{r_{ij}}\right)^n \frac{B_{ij}}{e^n} - \frac{A_{ij}}{r_{ij}^6} \quad (4)$$

approximation is based on the identity in eq 5 in which the logarithmic

$$\left(\frac{r_m}{r_{ij}}\right)^n \equiv \exp\left[-n \ln\left(\frac{r_{ij}}{r_m}\right)\right] \quad (5)$$

part is expanded around r_m as eq 6. When we drop the terms higher than

$$\ln\left(\frac{r_{ij}}{r_m}\right) = \frac{1}{r_m}(r_{ij} - r_m) - \frac{1}{2r_m^2}(r_{ij} - r_m)^2 + \frac{1}{3r_m^3}(r_{ij} - r_m)^3 - \ldots \quad (6)$$

the second in eq 6, substitute the remainder into eq 5, and rearrange the result, the exponential repulsion term in eq 3 can be expressed near r_m by eq 7. To speed the calculation, we replace the error function in eq

$$B_{ij}\exp(-C_{ij}r_{ij}) \approx \exp\left[-\frac{n}{2r_m^2}(r_{ij} - r_m)^2\right]\left(\frac{r_m}{r_{ij}}\right)^n \frac{B_{ij}}{e^n} \quad (7)$$

$$C_{ij} = n/r_m$$

7 by the Lorentzian function with the same half-width as

$$b = (2 \ln 2/n)^{1/2} r_m$$

and obtain eq 4. This potential is similar to the exp-6 type one near r_m ($=n/C_{ij}$) and approaches a Lennard-Jones n-6 potential in the range of smaller atomic distances. In the present work, the interaction energies between nonbonded atomic pairs separated by more than one atom were calculated by eq 4 in which n was set equal to 12. The potential parameters were taken from the set of Williams estimated on the basis of the crystal structures of hydrocarbons and aza hydrocarbons.[19] The approximate potentials calculated from this parameter set for the H···H and the C···C interactions are compared with the original exp-6 type potentials in Figure 1. The differences between the two potentials are negligible outside the distances of van der Waals contact. In contrast to the scheme of "foreshortening" used often in molecular mechanics calculations,[5,7] the interaction centers of hydrogen atoms were placed at the mass centers to avoid the lengthy readjustment of the dynamical matrix used in the normal-coordinate analysis. The geminal nonbonded atomic interactions were included in the calculation by using similar potential functions with a softer repulsion term ($n = 8$ and $b = r_m/2$) and the relevant parameters estimated separately.

The Coulomb potential includes the changes of atomic charges with the geometric structure by eq 8 where q_i^0 is the ith atomic charge when

$$q_i = q_i^0 + \sum_m \frac{\partial q_i}{\partial R_m} R_m \quad (8)$$

all the bond length and the valence angles are equal to their intrinsic values and $\partial q_i/\partial R_m$ is its flux defined as the derivative with respect to the mth internal coordinate. The Coulomb interactions between the atoms bonded to a common atom were assumed to be implicitly incorporated in the general valence-type force constants and were excluded from the pairwise sum. The first and the second derivatives of Coulomb potential (V_C) with respect to internal coordinates were calculated respectively by eq 9 and 10. In eq 10, the second derivatives of atomic charge ($\partial^2 q_i/\partial R_m \partial R_{m'}$) representing the electrical anharmonicity are neglected.

$$\frac{\partial V_C}{\partial R_m} = \frac{1}{\epsilon_{ij}}\left\{\sum_j \frac{\partial q_j}{\partial R_m}\sum_i q_i \rho_{ij} + \tfrac{1}{2}\sum_j q_j \sum_i q_i \frac{\partial \rho_{ij}}{\partial R_m}\right\} \quad (9)$$

$$\frac{\partial^2 V_C}{\partial R_m \partial R_{m'}} = \frac{1}{\epsilon_{ij}}\left[\sum_j \frac{\partial q_j}{\partial R_m}\sum_i \frac{\partial q_i}{\partial R_{m'}}\rho_{ij} + 2\sum_j \frac{\partial q_j}{\partial R_{m'}}\sum_i q_i \frac{\partial \rho_{ij}}{\partial R_m} + \tfrac{1}{2}\sum_j q_j \sum_i q_i \frac{\partial^2 \rho_{ij}}{\partial R_m \partial R_{m'}}\right] \quad (10)$$

$$\rho_{ij} = 1/r_{ij}$$

(19) Williams, D. E.; Cox, S. R. *Acta Crystallogr., Sect. B: Struct. Sci.* **1984**, *B40*, 404.

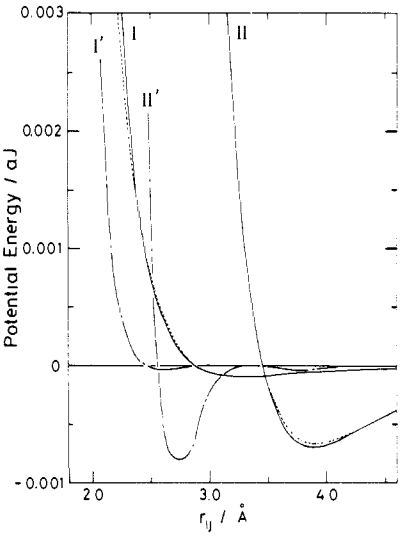

Figure 1. Comparison of the exchange repulsion–dispersion potentials: V_{Nb} (—); V_B (- - -); $V_{Nb} - V_B$ (-·-). I,I', H···H interaction; II,II', C···C interaction.

The numerical parameters in eq 1 for alkanes are summarized in Table I. All the intrinsic angles were commonly taken as tetrahedral; θ_0 = arccos (−1/3). The charge fluxes are shown in Table II. Their values were estimated by fitting the infrared intensity data as described in a later section.

Equilibrium Structures and Thermodynamic Functions. The internal coordinates in eq 1 are expressed as a power series of the Cartesian displacements of atoms up to the second order by using the coefficients of the curvilinear transformation between the internal and the difference Cartesian coordinates.[20] The first and the second derivatives of the potential function with respect to the Cartesian displacements of atoms, $\boldsymbol{F}_X$ and $\boldsymbol{F}_{XX}$, were then calculated by substituting eq 11 into eq 1. In this

$$R_i = \sum_k B_{ik} x_k + \tfrac{1}{2}\sum_{k,m} C_{ikm} x_k x_m \quad (11)$$

procedure, the number of nonvanishing eigenvalues of $\boldsymbol{F}_{XX}$ often exceeded the vibrational degrees of freedom because the linearized infinitesimal rotations of the whole molecule brought about molecular distortions in the second order, and certain forces resisting this distortion arose from the terms linear in R_i in eq 1 and the second-order coefficients C_{ikm} in eq 11. The contribution of the linearized molecular rotations to $\boldsymbol{F}_{XX}$ can be eliminated according to eq 12 where $\boldsymbol{B}_r$ and $(\boldsymbol{B}^{-1})_r$ are the rotational

$$(\boldsymbol{F}_{XX})_{in} = [\boldsymbol{E} - \tilde{\boldsymbol{B}}_r(\tilde{\boldsymbol{B}}^{-1})_r]\boldsymbol{F}_{XX}[\boldsymbol{E} - (\boldsymbol{B}^{-1})_r\boldsymbol{B}_r] \quad (12)$$

$\boldsymbol{B}$ matrix and the rotational submatrix of $\boldsymbol{B}^{-1}$, respectively. These matrices are defined in terms of the principal moment of inertia, I_x, I_y, I_z, the Cartesian coordinates of atoms in the principal axis system, X_1, Y_1, Z_1, ..., Y_N, Z_N, and the atomic masses, m_1, m_2, ..., m_N, as[21] in eq 13 and 14.

$$\boldsymbol{B}_r = \boldsymbol{M}^{-1/2}\boldsymbol{D}_r\boldsymbol{m} \quad (13)$$

$$(\boldsymbol{B}^{-1})_r = \boldsymbol{m}^{-1}\tilde{\boldsymbol{B}}_r = \tilde{\boldsymbol{D}}_r\boldsymbol{M}^{-1/2} \quad (14)$$

$$\boldsymbol{M} = \text{diag}\,[I_x I_y I_z]$$

$$\boldsymbol{D}_r = \begin{bmatrix} 0 & -Z_1 & Y_1 & 0 & -Z_2 & Y_2 & \ldots & 0 & -Z_N & Y_N \\ Z_1 & 0 & -X_1 & Z_2 & 0 & X_2 & \ldots & Z_N & 0 & -X_N \\ -Y_1 & X_1 & 0 & -Y_2 & X_2 & 0 & \ldots & -Y_N & X_N & 0 \end{bmatrix}$$

$$\boldsymbol{m} = \text{diag}\,[m_1 m_1 m_1 m_2 m_2 m_2 \ldots m_N m_N m_N]$$

The energy minimization was carried out by the Newton–Raphson method when $(\boldsymbol{F}_{XX})_{in}$ was positive semidefinite, and the steepest descent method, otherwise, until the stable geometry was reached. The normal frequencies were then calculated from the eigenvalues of $(\boldsymbol{F}_{XX})_{in}$ matrix at the potential minimum.

The heats of formation at 0 K, $\Delta H_f°$, were calculated from the potential minimum, and the zeropoint energy was obtained from the normal

(20) Machida, K. *J. Chem. Phys.* **1966**, *44*, 4186.
(21) Wilson, E. B., Jr.; Decius, J. C.; Cross, P. C. *Molecular Vibrations*; McGraw-Hill: New York, 1955.

Table I. Potential Parameters[a]

Bond Stretching			
r_i	a_i,[b] Å^{-1}	D_i,[c] aJ	r_i,[b] Å
C–H	1.8196	0.7308	1.095
C–C (C1–C1)	1.9452	0.5797	1.520
C–C (C2–C2)	1.9574	0.5970	1.520
C–C (C2–C2)[d]	1.9615	0.5945	1.520
C–C (C3–C3)	1.9135	0.6110	1.520
C–C (C3–C3)[d]	1.9166	0.6090	1.520
C–C (C4–C4)	1.8993	0.6205	1.520

Nonbonded Interaction			
r_{ij}	A_{ij},[c] aJ·Å^6	B_{ij},[c] aJ	C_{ij},[b] Å^{-1}
H···H	0.226	19.87	3.74
H···H (geminal)	0.226	1.46	3.02
C···C	4.049	613.69	3.60
C···C (geminal)	4.049	18.79	2.86

Torsion	
τ_{ijkl}	v_3, aJ
H–C–C–H	1.829×10^{-3}
H–C–C–C	1.329×10^{-3}
C–C–C–C	0.918×10^{-4}

General Quadratic (Diagonal)[e]

symbol	K_{aa}, aJ·rad^{-2}	symbol	K_{aa}, aJ·rad^{-2}
H_δ (H-C1-H)	0.5146	H_δ (H-C2-H)	0.5206
H_α (methane)	0.5010	H_γ, H_ζ (H-C2-C, H-C3-C)	0.5976
H_α (ethane)	0.5390	H_ω, H_ϕ, H_τ (C-C-C)	0.6779
H_β (H-C1-C2)	0.5522		
H_β (ethane)	0.6020		

General Quadratic (Off-Diagonal)[e,f]

symbol	K_{ab}
F_R (C–C, C–C; C common)	0.1307
$F_{R\gamma}$ (H–C–C, C–C; C–C common)	0.2147
$F_{R\omega}$ (C–C–C, C–C; C–C common)	0.2653
F_α (H–C–H, H–C–H; C–H common)[g]	–0.0250
F_γ (H–C–C, H–C–C; C–C common)	–0.0126
$F_{\gamma\omega}$ (H–C–C, C–C–C; C–C common)	0.0135
$F_{\gamma'}$ (H–C–C, H–C–C; C–H common)	0.0412
f_γ^t, f_γ^g (H–C–C, H–C–C)[h]	–0.1064 C_τ
$f_{\gamma\omega}^t$, $f_{\gamma\omega}^g$ (H–C–C, C–C–C)[h]	–0.1497 C_τ
f_ω^t, f_ω^g (C–C–C, C–C–C)[h]	–0.2181 C_τ

[a] C1, C2, C3, and C4 represent the carbon atoms of CH_3, CH_2, CH, and C groups, respectively. [b] The value for the pair X–Y is the arithmetic mean of those for the homogeneous pairs X–X and Y–Y. [c] The value for the pair X–Y is the geometric mean of those for the pairs X–X and Y–Y. [d] For cyclic alkanes. [e] The symbols of the force constants in ref 34 are used. [f] The stretch–stretch constant in N·cm^{-1}, stretch–bend constants in 10^{-8} N·rad^{-1}, and bend–bend constants in aJ·rad^{-2}. The same parameters are used for CH_3 group and branched alkanes. [g] Only for methane. [h] The dependence on the dihedral angle C–C–C–C is introduced by using a factor $C_\tau = \cos \tau_{CCCC}$.

frequencies according to the definition.[22] The standard heats of formation (at 298.15 K), ΔH_f, were obtained by using the enthalpy changes from 0 to 298.15 K caused by the thermal excitation to higher vibrational levels. The molar entropies were calculated from the translational, the rotational, and the vibrational partition functions. The last two functions were calculated on the basis of the rigid rotor–harmonic oscillator approximation by using the principal moment of inertia at the potential minimum and normal frequencies.[22]

Infrared Intensities. On the harmonic approximation, the integrated infrared intensity of the ith normal mode is given by eq 15 where n is the

$$A_i = \frac{1}{nl}\int_{\text{band } i} \ln (I_0/I)\, d\nu = \frac{N\pi g_i}{3c^2}\left(\frac{\partial \mu}{\partial Q_i}\right)^2 \qquad (15)$$

concentration (mol·cm^{-3}), l is the path length (cm), N is Avogadro's number, g_i is the degeneracy, c is light velocity (cm·s^{-1}), μ is the molecular dipole moment, and Q_i is the ith normal coordinate. The absorbance, $A(\nu)$, was calculated at every 1-cm^{-1} interval of the spectral range specified for each simulation by summing up the contributions from all the normal modes represented as Lorentzian functions in the form of eq 16 where ω_i is the half-bandwidth for the ith normal mode. To avoid

$$A(\nu) = [\ln (I_0/I)]_\nu = nl\sum_i \left[A_i \frac{2\omega_i}{\pi} \frac{1}{4(\nu - \nu_i)^2 - \omega_i^2} \right] \qquad (16)$$

too much flexibility in the parameterization at an early stage of the spectral simulation, we attributed a common value to all the ω_i's for each spectrum.

The components of the molecular dipole moment along the Cartesian coordinates are written as in eq 17 where $\xi_{3(k-1)+m}$ (m = 1–3) means x_k,

$$\mu_m = \sum_k q_k \xi_{3(k-1)+m} \qquad (17)$$

y_k, or z_k, and their derivatives with respect to Q_i are given by eq 18 where

(22) Rossini, F. D. *Chemical Thermodynamics*; Wiley: New York, 1950. Pitzer, K. S.; Gwinn, W. D. *J. Chem. Phys.* **1942**, *10*, 428.

Table II. Charge Fluxes[a,b]

Bond Stretching Fluxes, e·Å^{-1}			
$\partial q_H/\partial r_{CH}$	–0.216	$\partial q_H/\partial r_{CH}'$	–0.035
$\partial q_H/\partial R_{CC}'$	–0.030	$\partial q_C/s R_{CC}'$	+0.005
Angle Bending Fluxes, e·rad^{-1}			
CH_3 Group			
$\partial q_H/\partial \theta_{HCH}$	–0.003	$\partial q_H/\partial \theta_{HCC}$	–0.002
$\partial q_H/\partial \theta_{HCH}'$	+0.006	$\partial q_H/\partial \theta_{HCC}'$	+0.001
$\partial q_C/\partial \theta_{HCH}'$	–0.003	$\partial q_C/\partial \theta_{HCC}$	+0.003
CH Group			
$\partial q_H/\partial \theta_{HCC}$	–0.005	$\partial q_C/\partial \theta_{HCC}$	+0.010
$\partial q_H/\partial \theta_{CCC}'$	+0.005	$\partial q_C/\partial \theta_{HCC}'$	–0.005
CH_2 Group			
$\partial q_H/\partial \theta_{HCH}$	–0.005	$\partial q_C/\partial \theta_{HCC}$	+0.008
$\partial q_C/\partial \theta_{HCH}'$	+0.002	$\partial q_C/\partial \theta_{HCC}'$	–0.009
$\partial q_H/\partial \theta_{HCC}'$	–0.0025	$\partial q_H/\partial \theta_{CCC}'$	+0.010
CH_4			
$\partial q_H/\partial \theta_{HCH}$	–0.006	$\partial q_H/\partial \theta_{HCH}'$	+0.006

[a] e = electronic unit. [b] The unprimed internal coordinates are for the types $\partial q_i/\partial R_{ij}$ and $\partial q_i/\partial \theta_{ijk}$. The primed ones are for the types $\partial q_i/\partial R_{jk}'$ (i is bonded to j or k) and $\partial q_i/\partial \theta_{jkm}'$ (i is bonded to k).

Table III. Experimental and Calculated Heats of Formation[a]

	0 K		298.15 K	
molecule	exptl[b]	calcd	exptl[c]	calcd
methane	–66.9	–65.2	–74.4	–73.2
ethane	–69.1	–69.4	–83.8	–85.1
propane	–81.6	–81.9	–104.7	–104.4
n-butane	–99.1	–97.3	–125.6	–126.1
isobutane	–105.9	–105.4	–134.2	–134.3
n-pentane	–114.2	–111.9	–146.9	–146.9
isopentane	–120.6	–117.7	–154.5	–152.1
neopentane	–131.0	–132.8	–168.1	–168.3
n-hexane	–129.8	–126.5	–167.1	–167.4
2-methylpentane	–134.3	–130.5	–174.8	–171.9
3-methylpentane	–133.8	–128.4	–172.1	–169.5
2,2-dimethylbutane	–145.0	–140.7	–186.1	–183.2
2,3-dimethylbutane	–137.0	–130.6	–178.3	–172.9
n-heptane	–144.6	–141.3	–187.7	–188.3
n-octane	–159.9	–155.9	–208.6	–208.9
cyclopentane[d]	–44.7	–41.2	–76.4	–74.8
cyclohexane	–83.8	–81.2	–123.4	–120.7
methylcyclohexane	–110.1	–107.4	–154.7	–152.8
1,1-dimethylcyclohexane	–129.5	–128.2	–180.9	–180.1
cycloheptane			–118.1	–121.5
cyclooctane			–124.4	–123.3
cis-decalin			–169.2	–173.3
trans-decalin			–182.2	–179.6

[a] In kJ·mol^{-1}. [b] Rossini, F. D.; Arnett, R. L.; Braum, R. M.; Pimentel, G. C. *Selected Values of Physical and Thermodynamic Properties of Hydrocarbons and Related Compounds*; Carnegie: Pittsburgh, PA, 1953. [c] Pedley, J. B.; Naylor, R. D.; Kirby, S. P. *Thermochemical Data of Organic Compounds*, 2nd ed.; Chapman and Hall: London, 1986. [d] The C···C nonbonded interaction energy was calculated by average of the potentials for geminal and vicinal interactions.

q_k^e is the atomic charge at the equilibrium geometry, R_j is the jth internal coordinate, and $(L_x)_{pq}$ is the pq element of the L_x matrix. Decius[23] first

$$\frac{\partial \mu_m}{\partial Q_i} = \sum_k \left[\xi_{3(k-1)+m} \sum_j \frac{\partial q_k}{\partial R_j} \sum_n B_{jn}(L_x)_{n,i} + q_k^e (L_x)_{3(k-1)+m,i} \right] \quad (18)$$

proposed the use of q_k^e and $\partial q_k/\partial R_j$ as the infrared intensity parameters and called them the equilibrium charges and the charge fluxes. In this work, we calculated q_k at each iteration step of energy minimization according to eq 8, and q_k^e was obtained as the atomic charge for the optimized structure at the final step of the iteration. In this way, q_k^0 and $\partial q_k/\partial R_j$ are made exactly the common parameters in the potential function (eq 1) and in the simulation of infrared spectra. Since the higher order terms are neglected, eq 8 is valid only for small values of R_m. It may be necessary to modify q_k^0 when an internal coordinate undergoes a large change as in the case of the conformational change between the trans and the gauche conformers.

Mast and Decius[24] estimated the equilibrium charges on the hydrogen and carbon atoms in methane as +0.064 and −0.256e, respectively, from the analysis of the infrared intensities. Gussoni et al. calculated the electrooptical parameters, i.e., the bond moments and their derivatives with respect to internal coordinates, for n-alkanes, ethylene, acetylene, polyethylene, and aldehydes[11-16,25] and examined the transferability of these parameters. They suggested that the bond moments were linearly related to the difference of electronegativities between the bonded atoms and that the equilibrium charge on hydrogen derived from the bond dipoles was between +0.04 and +0.06e.[14,16] Inclusion of effective charges in molecular mechanics has been attempted by several authors.[2,8] The charges adopted in an earlier force field of Warshel and Lifson[2] are too large while those introduced in MM2 by Allinger[8] are too small to elucidate the infrared intensity data.

Considering these circumstances, we estimated the values of q_k^0 from the electronegativities[26] by a single formula (eq 19) where n is the number

$$q_k^0 = \sum_i^n \beta(\chi_i - \chi_k) \quad (19)$$

of atoms bonded to the atom k and β is an adjustable parameter to be determined from any known atomic charges. If we adopt a common value of β in eq 19, the positive charges on hydrogen atoms are made uniform, while the negative charges on the carbon atoms of methyl, methylene, and methine groups are in the ratio 3:2:1. This charge distribution leads to exactly vanishing dipole moments of propane and isobutane. The microwave data indicate, however, that propane and isobutane have small but nonnegligible dipole moments[27,28] with the methyl groups at the negative end.[29] To reproduce these dipole moments and their directions without breaking the homogeneity of the hydrogen charges, we should reinforce the unbalance of the charges among the carbon atoms of methyl and methylene groups. However, the charge unbalance among the carbon atoms of methyl and methylene groups results in an appreciable overestimation of the intensities of the infrared bands involving the motions of methyl groups. To avoid such unbalance of charges among the carbon atoms and to reproduce the observed dipole moments, the hydrogenic charges of methyl, methylene, and methine groups are assumed to be +0.04e (β = 0.100), +0.05e (β = 0.125), and +0.06e (β = 0.150), respectively. The atomic charges obtained by this method are closer to those derived by del Re's method[30] and by the ab initio MO method with the STO3G basis set than those calculated by the CNDO method. Gussoni et al. pointed out that the CNDO charges were inadequate to predict the infrared intensities.[16]

The charge fluxes were introduced for the stretching and bending coordinates. The bond-stretching fluxes were attributed to the terminal atoms ($\partial q/\partial r$) and the atoms bonded to them ($\partial q/\partial r'$), while the angle bending fluxes to the three constituent atoms, one apex atom and two anchors ($\partial q/\partial \theta$), and the atoms bonded to the apex atom ($\partial q/\partial \theta'$). From the electrical neutrality conditions, the bending charge flux at the apex atom should be expressed as eq 20. Moreover, the redundancy among

$$\frac{\partial q_j}{\partial \theta_{ijk}} = -\left[\frac{\partial q_i}{\partial \theta_{ijk}} + \frac{\partial q_k}{\partial \theta_{ijk}} + \sum_m \frac{\partial q_m}{\partial \theta_{ijk'}} \right] \quad (20)$$

(23) Decius, J. C. *J. Mol. Spectrosc.* **1975**, *57*, 348.
(24) Mast, G. B.; Decius, J. C. *J. Mol. Spectrosc.* **1980**, *79*, 158.
(25) Castiglioni, C.; Gussoni, M.; Zerbi, G. *J. Chem. Phys.* **1985**, *82*, 3534.
(26) Pauling, L. *The Nature of the Chemical Bond*; Cornell University: Ithaca, NY, 1960.
(27) Lide, D. R. *J. Chem. Phys.* **1960**, *33*, 1514.
(28) Lide, D. R. *J. Chem. Phys.* **1958**, *29*, 914.
(29) Muenter, J. S.; Laurie, V. W. *J. Chem. Phys.* **1966**, *45*, 855.
(30) del Re, G. *J. Chem. Soc.* **1958**, 4031.

Table IV. Experimental and Calculated Molar Entropies[a]

molecule	temp, K	exptl	calcd
methane	298.15	0.186[b]	0.186
ethane	184.1	0.207[c]	0.207
propane	231.09	0.253[d]	0.253
n-butane	272.65	0.302[e]	0.293
isobutane	261.43	0.283[f]	0.282
n-pentane	298.15	0.350[b]	0.333
isopentane	298.15	0.344[b]	0.342
neopentane	282.61	0.298[g]	0.298
n-hexane	298.15	0.389[b]	0.364
cyclohexane	298.15	0.298[b]	0.301
n-octane	298.15	0.467[b]	0.428

[a] In kJ·deg^{-1}·mol^{-1}. [b] Reference b in Table III. [c] Witt, R. K.; Kemp, J. D. *J. Am. Chem. Soc.* **1937**, *59*, 273. [d] Kemp, J. D.; Egan, C. J. *J. Am. Chem. Soc.* **1938**, *60*, 1521. [e] Aston, J. G.; Messerley, G. H. *J. Am. Chem. Soc.* **1940**, *62*, 1917. [f] Aston, J. G.; Kennedy, R. M.; Schumann, S. C. *J. Am. Chem. Soc.* **1940**, *62*, 2059. [g] Enokido, H.; Shinoda, T.; Mashiko, Y. *Bull. Chem. Soc. Jpn.* **1969**, *42*, 84.

Table V. Experimental and Calculated Structure Parameters[a]

molecule	param	exptl	calcd
propane	r_{CC}	1.532[b]	1.533
	θ_{CCC}	112.0	112.4
isobutane	r_{CC}	1.535[c]	1.537
	θ_{CCC}	110.8	111.0
cyclohexane	r_{CC}	1.536[d]	1.541
	θ_{CCC}	111.4	111.6
	τ_{CCCC}	54.9	54.5
cyclooctane	r_{CC}^{av}	1.540[e]	1.543
	θ_{CCC}^{av}	116.8	116.3
	τ_{1234}	−98.0	−98.6
	τ_{2345}	42.0	42.3
	τ_{3456}	68.3	62.0
	τ_{4567}	−68.3	−62.0
	τ_{5678}	−42.0	−42.3
	τ_{6781}	98.4	98.6
	τ_{7812}	−63.1	−69.4
	τ_{8123}	63.1	69.4

[a] Distances in Å; angles in deg. [b] Iijima, T. *Bull. Chem. Soc. Jpn.* **1972**, *45*, 1291. [c] Hilderbrandt, R. L.; Wieser, J. D. *J. Mol. Struct.* **1973**, *15*, 27. [d] Bastiansen, O.; Fernholt, L.; Seip, H. M.; Kambara, H.; Kuchitsu, K. *J. Mol. Struct.* **1973**, *18*, 163. [e] For numbering, see ref 38.

the six bending coordinates around a sp^3 carbon atom leads to the relation in eq 21. The charge fluxes in Table II were thus obtained by fitting

$$\sum_{j=1}^{6} \frac{\partial q_i}{\partial \theta_j} = 0 \quad (21)$$

the intensity data and infrared spectra of ethane through n-hexane. The flux for the C–H bond is the same as that derived from the bond dipole proposed by Gussoni et al.,[11,13] but those for the bending coordinates are different from their values, because our model is simplified by neglecting the charge fluxes of the atoms bonded to the anchor atoms of the bending coordinates.

A computer program was written for an automatic specification of the internal coordinates, the potential parameters, and the intensity parameters. The input required for the calculation is the atomic numbers of the constituent atoms and their Cartesian coordinates.

Results and Discussion

The observed and calculated heats of formation of simple alkanes are compared with each other in Table III. The observed heats of formation of branched alkanes are appreciably smaller than those of n-alkanes. In most of the currently used molecular mechanics calculations, these differences are reproduced by setting different values of the energy increments for methyl, *sec*-alkyl, and *tert*-alkyl groups, and the vibrational contribution to the heats of formation are included implicitly in these parameters.[7,9,10] In the present work, the heat of formation of each molecule was calculated from the depth of the potential minimum, the zeropoint energy, and the thermal contributions of the vibrational excited states, and the entropies were calculated from the principal moments of inertia and normal frequencies by following the standard

Table VI. Normal Frequencies and Infrared Absorption Intensities of Methane, Ethane, and Their Deuteriated Derivatives

molecule	ν, cm^{-1}		A_i[a]	
	exptl[b]	calcd	exptl	calcd
CH_4[c]	3019	3053	6728	6744
	1306	1309	3364	3351
CH_3D[c]	3021, 2945	3053, 2989	4919	5189
	2200	2229	628	589
	1471 ~ 1155	1474 ~ 1155	2923	3058
CH_2D_2[c]	3013, 2976	2992, 2952	3484	3748
	2234, 2202	2232, 2140	1383	1396
	1234 ~ 1033	1236 ~ 1033	2146	2190
CHD_3[c]	2993	2973	1570	1908
	2200, 2142	2231, 2095	2093	2278
	1291	1295	665	697
	1036, 1003	1033, 1007	1523	1563
CD_4[c]	2259	2274	2609	3038
	996	984	1936	2028
CH_3CH_3[d]	2995	2978	12318	13737
	2915	2863	4780	4963
	1472	1477	1340	1319
	1379	1404	410	557
	821	828	610	570
CH_3CH_2D[e]	~2900	2978 ~ 2884	14600	15546
	2184	2178	1400	1553
	~1400	1482 ~ 1399	1290	1321
	~1310	1307, 1305	350	446
	~1140	1168, 1118	80	74
	978	969	20	20
	804	814	380	307
	713	716	160	173
CH_3CD_3[e]	~2900	2976, 2910	9260	9149
	2240	2222	3030	3543
	2090	2091	1370	1366
	~1400	1481, 1399	950	947
	~1100	1123, 1067	660	667
	904	895		22
	673	680	420	357
CD_3CD_3[d]	2236	2212	6440	6969
	2095	2056	2420	2394
	1082	1069	912	851
	1077	1074	291	370
	594	528	331	296

[a] In 10^3 cm·mol^{-1}. [b] X, Y and $X \sim Y$ indicate that two and more than two bonds are not resolved in the intensity data, respectively. [c] Observed data from: Hiller, R. E.; Straley, J. W. *J. Mol. Spectrosc.* **1960**, *5*, 24. [d] Observed data from: Nyquist, I. M.; Mills, I. M.; Person, W. B.; Crawford, B. *J. Chem. Phys.* **1957**, *26*, 552. [e] Observed data from: Kondo, S.; Saeki, S. *Spectrochim. Acta, Part A* **1973**, *29A*, 735.

procedure of statistical mechanics rigorously.[22] The only approximation introduced was to incorporate the torsional motions around the C–C bonds in the vibrational degrees of freedom. According to Chalk et al.,[31] the molar entropies calculated from this approximation are in better agreement with the experimental values than those calculated from the approximation of free internal rotation. The observed heat of formation of neopentane at 0 K is 16.87 kJ·mol^{-1} lower than that of *n*-pentane, while the difference in zero-point energies is only 2.71 kJ·mol^{-1} (3.06 kJ·mol^{-1} from the frequencies calculated by Snyder et al.[38,39]). Within the framework of the present potential model, the Coulomb attraction between the vicinal C–H pair mainly contributes to the stabilization of neopentane. When the vicinal Coulomb interaction terms are neglected completely, the difference in the heat of formation between neopentane and *n*-pentane was calculated to be only 3.51 kJ·mol^{-1}. On taking account of this interaction to the full extent, however, we obtained an exaggerated splitting of the torsional frequencies around the C–C bonds. Both these defects of the potential could be removed by modifying the coulombic terms for vicinal atom pairs with an apparent dielectric constant $\epsilon_{ij} = 1.65$. The parameters of the Morse potential for the C–C bonds were slightly changed according to the bond type

(31) Chalk, C. D.; Hutley, B. G.; McKenna, J.; Sims, L. B.; Williams, I. H. *J. Am. Chem. Soc.* **1981**, *103*, 260.

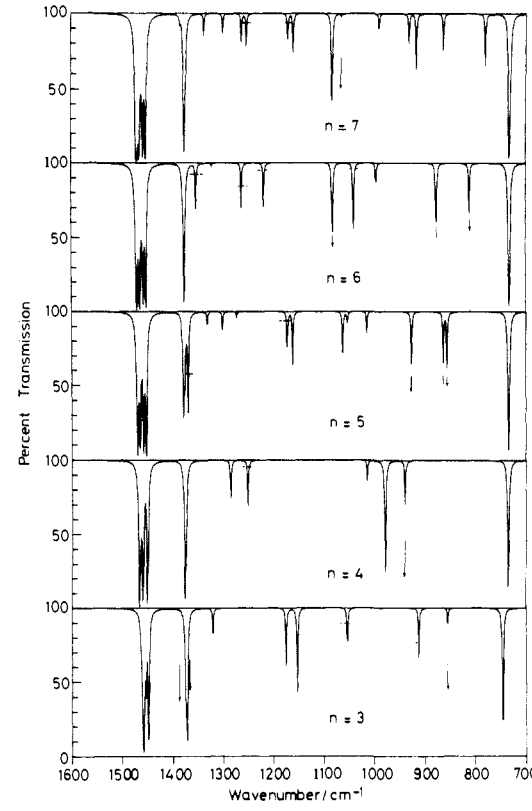

Figure 2. Simulated infrared spectra of n-C_nH_{2n+2} in all-trans form. $nl = 1.5 \times 10^{-5}$ mol·cm^{-2}.

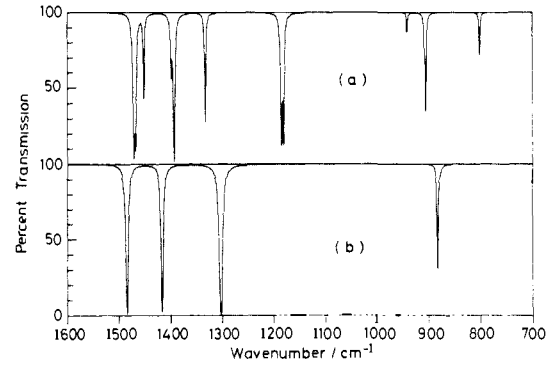

Figure 3. Simulated infrared spectra of isobutane (a) and neopentane (b). $nl = 1.5 \times 10^{-5}$ mol·cm^{-2}.

as shown in Table I to correct for the residual difference left unexplained with this Coulomb interaction energy. To reproduce the heats of formation of macrocyclic alkanes whose valence angles are unusually extended from the intrinsic value, θ_i^0, both the inclusion of the geminal nonbonded interaction potential and the reduction of the diagonal force constants, H_j, for the bending potential in eq 1 were necessary. By these adjustments, the calculated heats of formation of alkanes listed in Table III were made consistent with the observed data within ±2.7 kJ·mol^{-1}.

In Table IV the entropies calculated from the present potential are compared with the experimental values. The agreements are sufficient for small alkanes, but the systematic errors due to the underestimation of the torsional contribution arising from the harmonic approximation turn out to be appreciable in the calculated entropies of larger molecules.

The rotational barrier of ethane with the present potential, 12.20 kJ·mol^{-1}, is very close to the value of 12.26 kJ·mol^{-1} estimated from the infrared torsional spectra.[32] However, the calculated enthalpy difference between the trans and the gauche isomers of *n*-butane, 2.19 kJ·mol^{-1}, was appreciably lower than the observed

(32) Weiss, S.; Leroi, G. E. *J. Chem. Phys.* **1968**, *48*, 962.

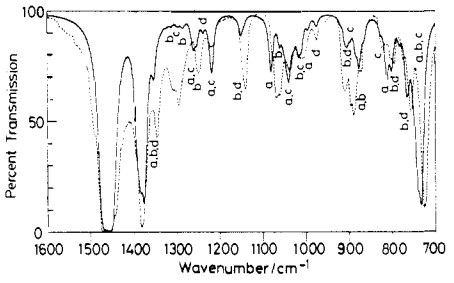

Figure 4. Simulated (solid line) and observed (broken line) infrared spectra of *n*-hexane in the liquid state (d = 0.660) at room temperature. The symbols a–d represent the conformers TTT, TTG, TGT, and TGG, respectively (T = trans and G = gauche[43]). The spectrum was measured with a Jasco IRA-2 IR spectrometer: slit width 1.5 cm^{-1} at 1000 cm^{-1}; path length 0.1 mm.

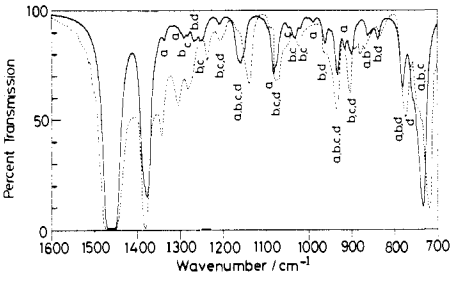

Figure 5. Simulated (solid line) and observed (broken line) infrared spectra of *n*-heptane in the liquid state (d = 0.684) at room temperature. The symbols a–d represent the conformers TTTT, TTTG, TTGT, and TTGG, respectively. For the experimental conditions, see caption of Figure 4.

value in the gaseous state, 3.72 kJ·mol^{-1}.[33] The free energy difference between axial and equatorial methylcyclohexane was calculated to be 4.55 kJ·mol^{-1} at 172 K. This value is also lower than the experimental value, 7.28 kJ·mol^{-1}.[34] On the other hand, the enthalpy differences among various rotamers of *n*-alkanes calculated by the present potential are close to the experimental values in the liquid state[35] and the recent value for *n*-pentane in the gaseous state.[36]

The calculated structure parameters for typical alkanes are summarized in Table V. The calculated C–C–C angles at the potential minimum are extended from the intrinsic tetrahedral value by the repulsive forces of the van der Waals and Coulomb interactions and agree well with the experimental values. The geometry of cyclohexane in the chair conformation is very accurately reproduced by the calculation. As shown in Table V, the calculated structure parameters for cyclooctane in the boat–chair conformation are in agreement with the experimental as well as the calculated values by Dorofeeva et al.[37]

Normal frequencies are important not only for the simulation of vibrational spectra but also for the calculation of the thermodynamic quantities. The charge fluxes included in the present potential except for the C–H bond stretching flux, $\partial q_H/\partial r_{CH}$, do not give rise to any changes of the calculated frequencies greater than 10 cm^{-1}. The inclusion of $\partial q_H/\partial r_{CH}$ decreases the frequencies of methyl and methylene C–H symmetric stretching modes of *n*-alkanes from 2900 to 2850 cm^{-1}, which is close to the observed value 2860 cm^{-1}. When this charge flux is neglected, no simultaneous fit between the calculated and the experimental values of the torsional frequency and the barrier height of ethane can be achieved without supplementing $V_1(\tau_{ijkl})$ with a sixfold potential.

$$V_6 = \frac{1}{2}v_6(1 + \cos 6\tau_{ijkl})$$

The present force field yields normal frequencies that are a little less accurate than those derived from the well-refined force fields exclusively adapted for the normal-coordinate analysis.[38–40] The standard deviation below 1500 cm^{-1} for *n*-butane through *n*-hexane, cyclohexane, and their deuteriated derivatives in this work is ±10.2 cm^{-1}, while the deviations for *n*-butane through *n*-hexane[38] and for cyclohexane[39] in Snyder's force field are ±4.7 and ±14.8 cm^{-1}, respectively, and the deviation for *n*-butane through *n*-hexane and their deuteriated derivatives in the local symmetry force field[40] is ±4.2 cm^{-1}.

The infrared absorption intensities of simple alkanes were calculated by using the final atomic charges after energy minimization and the charge fluxes in Table II, and the infrared spectra were simulated with these intensities. As mentioned above, the hydrogenic atomic charges of methyl, methylene, and methine groups were taken to be +0.04, +0.05, and +0.06e, respectively. From this charge distribution, the dipole moments of propane and isobutane were calculated to be 0.078 and 0.125 D, respectively, which are consistent with the respective experimental data, 0.083 and 0.132 D.[27,28] This order of hydrogen charges is also consistent with that of the proton chemical shifts for the alkyl groups in NMR spectra.[41] The hydrogen charge of methane is considered to be smaller than +0.04e from the proton chemical shift. However, this charge could not be determined uniquely from the infrared intensities alone, since the intensities can be adjusted by the combination of charge and charge fluxes. In this work, the hydrogen charge of methane was assumed to be +0.04e and $\partial q_H/\partial r_{CH}$ was modified to be −0.200 e·Å^{-1}. As shown in Table VI, the absolute intensities of methane, ethane, and their deuteriated derivatives agree well with the experimental intensities.

The infrared spectra of propane and fully extended *n*-butane through *n*-heptane are simulated with the constant half-width of 2 cm^{-1} in Figure 2. To facilitate comparison with the observed spectra,[42] those bands calculated to be too intense and too weak compared to the CH_2 in-phase rocking band near 720 cm^{-1} are marked with horizontal dotted lines and vertical arrows, respectively. The horizontal lines and the arrowheads indicate the observed heights. In the spectrum of propane, the two observed bands at 1389 (A_1) and 1370 (B_1) cm^{-1}, which arise from methyl symmetric bending modes, are overlapped in the simulated spectrum, since the calculated separation is only 3 cm^{-1}. In the observed spectrum of *n*-butane,[42] the absorption due to the methyl symmetric bending is split into three bands (1379, 1368, and 1364 cm^{-1}). The intensity of the calculated band at 1375 cm^{-1} corresponds roughly to the sum of the three observed bands. In other respects, no systematic discrepancies are found throughout the simulated *n*-alkanes and the overall patterns agree well with the observed spectra. The simulated spectra of isobutane and neopentane are shown in Figure 3. The calculated spectral patterns represent well the observed spectra in the solid state,[39] but the calculated frequencies of two bands between 1250 and 1450 cm^{-1} of neopentane are about 50 cm^{-1} higher than the observed frequencies. These discrepancies result from the overestimation of the second derivatives of the exchange repulsion potential between nonbonded atomic pairs and can be adjusted by modifying some quadratic force constants of alkyl groups connected to the quaternary carbon. We used, however, the force constants refined for *n*-alkanes commonly for branched alkanes to avoid complicated indexing of force constants at the starting point. More detailed specifications of these constants would be necessary for fitting

(33) Compton, D. A. C.; Montero, S.; Murphy, W. F. *J. Phys. Chem.* **1980**, *84*, 3587.
(34) Booth, H.; Everett, J. R. *J. Chem. Soc., Chem. Commun.* **1976**, 278.
(35) Harada, I.; Takeuchi, H.; Sakakibara, M.; Matsuura, H.; Shimanouchi, T. *Bull. Chem. Soc. Jpn.* **1977**, *50*, 102.
(36) Kanesaka, I.; Snyder, R. G.; Strauss, H. L. *J. Chem. Phys.* **1986**, *84*, 395.
(37) Dorofeeva, O. V.; Mastryukov, V. S.; Allinger, N. L.; Almenningen, A. *J. Phys. Chem.* **1985**, *89*, 252.
(38) Schachtschneider, J. H.; Snyder, R. G. *Spectrochim. Acta* **1963**, *19*, 117.
(39) Snyder, R. G.; Schachtschneider, J. H. *Spectrochim. Acta* **1965**, *21*, 169.
(40) Shimanouchi, T.; Matsuura, H.; Ogawa, Y.; Harada, I. *J. Phys. Chem. Ref. Data* **1978**, *7*, 1323.
(41) Cavanaugh, J. R.; Dailey, B. P. *J. Chem. Phys.* **1961**, *34*, 1099.
(42) Snyder, R. G.; Schachtschneider, J. H. *Spectrochim. Acta* **1963**, *19*, 85.
(43) Shimanouchi, T.; Ogawa, Y.; Ohta, M.; Matsuura, H.; Harada, I. *Bull. Chem. Soc. Jpn.* **1976**, *49*, 2999.

the normal frequencies of branched alkanes as accurately as *n*-alkanes.

The relative populations of rotational isomers of *n*-hexane and *n*-heptane at 298.15 K were calculated from the ΔG's among these isomers obtained from the present force field and neglecting the intermolecular interactions.[17] The integrated intensities of normal modes for the rotational isomers whose populations were larger than 5% were calculated and the absorbance of the mixture at wavenumber ν, $A_m(\nu)$, were calculated by eq 22 where $A_k(\nu)$ and

$$A_m(\nu) = \sum_k p_k A_k(\nu) \qquad (22)$$

p_k are the absorbance and the population, respectively, of the kth isomer, the former being calculated by eq 16. The simulated spectra of *n*-hexane and *n*-heptane are compared with the observed spectra in the liquid state at room temperature in Figures 4 and 5, respectively, where the conformers contributing to the intensity of individual simulated bands are shown. The half-bandwidth for these simulated spectra was assumed to be 10 cm^{-1} from the observed value of the isolated band at 1140 cm^{-1} of *n*-hexane. When this half-width was used, the heights of the CH_2 rocking bands near 720 cm^{-1} agreed well with observed heights. The simulated band at 1140 cm^{-1} in the spectrum of *n*-hexane and those near 1300 cm^{-1} in both the spectra due to gauche conformers are too weak compared with the observed bands. The enthalpy differences among the rotamers of *n*-hexane calculated by the present potential agreed well with the observed values in the liquid state.[17] Therefore, these disagreements may be caused by the inadequacies of a part of intensity parameters for gauche conformers. According to a preliminary calculation, the underestimated intensities of the bands due to the gauche conformers can be enhanced by increasing the intrinsic atomic charge of the hydrogen in the C-C-C plane, which includes the gauche C-C bond, and by adding a negative charge flux on this hydrogen with respect to the ∠HCC bending coordinate. These modifications of the intensity parameters seem to be favorable also for fitting the spectra of cyclohexane and its deuteriated derivatives, but more extensive work is necessary for estimating their best values. In other respects, the simulated spectra explain the appearance of many bands assignable to different rotamers on the change of state.

The reproduction of the thermodynamic functions and the structure parameters of alkanes and the success of simulations of infrared spectra of *n*-alkanes show that the atomic charges and charge fluxes assumed in this work can be used simultaneously as the potential parameters and the infrared intensity parameters. Extention of this approach to more polar molecules is now in progress.

Acknowledgment. This work was supported by a Grant-in-Aid for Scientific Research (No. 62570964) from the Ministry of Education, Science and Culture. The calculation in this work was performed on FACOM M-780 and FACOM VP-200 computer systems in the Data Processing Center, Kyoto University.

Communications to the Editor

Reactivities of Ester Radical Anions

John Masnovi* and Jeanne Maticic

Department of Chemistry, Cleveland State University Cleveland, Ohio 44115

Received November 9, 1987

A common reaction of radical anions is decomposition to produce an anion and a radical fragment.[1-3] The rate of this process determines the efficiency of many reactions, such as electron-transfer quenching of excited states, in which the initial electron transfer is reversible.

Our interest in reactions that are driven by dissociative electron transfer[4-6] led us to examine the reduction of esters of carboxylic acids. Alkyl benzoates in 2% ethanolic 2-propanol quench the absorption of solvated electrons ($\lambda_{MAX} \sim 700$ nm[7]), generated by pulse radiolysis,[8] with rate constants $k_e = (5 \pm 1) \times 10^9$ M^{-1} s^{-1}. Two transient absorption bands, appearing at 310 nm ($\epsilon \sim 35000$ M^{-1} cm^{-1}) and 445 nm ($\epsilon \sim 9500$ M^{-1} cm^{-1}), form si-

Table I. Rates of Decomposition of Ester Radical Anions

substrate	k (s^{-1})[a] alcohol (λ_{MON})[b]	hexane (λ_{MON})[b]
$CH_3OCOC_6H_5$	5×10^3 (310, 445)	4.1×10^4 (305, 440)
$CH_3CH_2OCOC_6H_5$	5×10^3 (310, 445)	4.1×10^4 (305, 440)
$C_6H_5CH_2OCOC_6H_5$	4.8×10^4 (310, 445)	2.2×10^5 (440)
$(C_6H_5)_2CHOCOC_6H_5$	4.6×10^5 (330,[d] 450)	5×10^6[c] (330,[d] 440)
C_6H_4-*o*-$(COOCH_2CH_3)_2$	$\leq 1 \times 10^3$[e] (340, 780)	$\sim 4 \times 10^4$[e] (330)
$C_6H_5COOCOC_6H_5$	*f*	3.2×10^5 (300, 450)
$C_6H_5CH_2OCOCH_3$	1.4×10^6 (310[d])	$\geq 2 \times 10^6$[c]
$(C_6H_5)_2CHOCOCH_3$	$>2 \times 10^6$[c] (330[d])	$\geq 5 \times 10^6$[c]

[a] Decay of radical anions at 22 ± 1 °C. [b] Monitoring wavelength(s), nm. [c] Rates greater than experimental resolution. [d] Growth of radical monitored (k or k'). [e] Decay nonexponential even at low OD. [f] Not determined.

(1) (a) Andrieux, C. P.; Savéant, J.-M.; Su, K. B. *J. Phys. Chem.* **1986**, *90*, 3815. (b) Prasad, D. R.; Hoffman, M. Z.; Mulazzani, Q. G.; Rodgers, M. A. J. *J. Am. Chem. Soc.* **1986**, *108*, 5132. (c) Maslak, P.; Guthrie, R. D. *J. Am. Chem. Soc.* **1986**, *108*, 2628. Lan, J. Y.; Schuster, G. B. *Ibid.* **1985**, *107*, 6710.

(2) (a) Wade, P. A.; Morrison, H. A.; Kornblum, N. *J. Org. Chem.* **1987**, *52*, 3102. (b) Neta, P.; Behar, D. *J. Am. Chem. Soc.* **1981**, *103*, 103.

(3) Hamill, W. H. *Radical Ions*; Kaiser, E. T., Kevan, L., Eds.; Interscience: New York, 1968; Chapter 9, pp 408-412.

(4) Masnovi, J.; Koholic, D. J.; Berki, R. J.; Binkley, R. W. *J. Am. Chem. Soc.* **1987**, *109*, 2851.

(5) Masnovi, J. M.; Kochi, J. K.; Hilinski, E. F.; Rentzepis, P. M. *J. Am. Chem. Soc.* **1986**, *108*, 1126. Masnovi, J. M.; Huffman, J. C.; Kochi, J. K.; Hilinski, E. F.; Rentzepis, P. M. *Chem. Phys. Lett.* **1984**, *106*, 20.

(6) Masnovi, J. M.; Kochi, J. K. *J. Am. Chem. Soc.* **1985**, *107*, 6781.

(7) Taub, I. A.; Harter, D. A.; Sauer, M. C., Jr.; Dorfman, L. M. *J. Chem. Phys.* **1964**, *41*, 979.

(8) For a description of the radiolysis apparatus, see: Atherton, S. J. *J. Phys. Chem.* **1984**, *88*, 2840. Foyt, D. C. *Comput. Chem.* **1981**, *5*, 49. Rodgers, M. A. J.; Foyt, D. C.; Zimek, Z. A. *Radiat. Res.* **1978**, *75*, 296. Phthalate esters are used as plasticizers; therefore, the apparatus was assembled entirely from glass. A variable pulse width was employed to test kinetic order. A pulse of ≥100 ns was found necessary to produce sufficient signal for analyses. Concentration of esters routinely was made 2 mM so that reaction of the electrons occurred mostly within the pulse. The decays did not depend upon concentration of ester. The decays monitored at 310 nm are more complex than are those at 445 nm. Other, persistent absorbing species (reaction products and species derived from solvent[9]) also have absorptions in the 300-nm region, and the decays monitored at 310 nm do not approach baseline. Kinetics at 310 nm, determined by the method of initial rates and accounting for residual absorption, agreed with those determined at 445 nm within experimental error (±30%); e.g., see Table I, entry 4 and Figure 1c. Decays at 445 nm had standard deviations ≤20% (100 ns pulse); however, a dependence on the pulse width and analysis of residuals for the slower decays ($< \sim 10^4$ s^{-1}) indicated the kinetics in these cases were not simple first-order. Extinction coefficients of the radical anions were estimated by comparison of the signal intensities observed for benzyl radical products[10,11] and agreed with those calculated by dosimetry. Products were determined by GC and GC/MS.

0002-7863/88/1510-5189$01.50/0